ESO Science Archive Facility - Phase 3 Data Release Description
ESO programme 3D Mapping of the Dynamic Feedback and Chemistry in the Star Formation Process across Galaxy Disks, Data Release DR1.1
provided by E. Schinnerer, published on 2025-05-14
release description document revised on 2025-05-14

The PHANGS-MUSE Nebula Catalog

Abstract

We present the **PHANGS–MUSE Nebular Catalogue**, a value-added data release based on integral-field spectroscopic observations of **19 nearby star-forming disk galaxies** conducted as part of the **PHANGS–MUSE Large Programme** (ESO **1100.B-0651**; PI Schinnerer). These observations are supplemented by data from ESO programmes **094.C-0623, 095.C-0473 and 098.C-0484**, as well as archival data from five additional programmes: **094.B-0321** (*MAGNUM*), **099.B-0242**, **0100.B-0116**, **098.B-0551** (*MAD*), and **097.B-0640** (*TIMER*). All observations were performed with the **MUSE instrument on the VLT** in Wide Field Mode, covering a nominal wavelength range of ~4750–9350 Å. The survey combines AO and non-AO pointings to build mosaicked datacubes for each galaxy.

The survey delivers **high-resolution (~70 pc)** spectroscopic maps of galaxy disks, obtained under typical seeing conditions of 0.7″ to 1.0″. Each galaxy field is constructed from multiple MUSE pointings, carefully mosaicked and PSF-matched across wavelength and position. From these mosaics, we identify and catalogue a total of **31,399 sources**, **of which 30,790 are reliable ionized nebulae (i.e. without edge flags)**, the majority of which (~75%) are classified as **H II regions**, using a modified version of the **HIIphot algorithm** applied to Hα emission maps. For each nebula, we provide **integrated emission-line measurements** and a suite of **derived physical properties**, including **attenuation**, **metallicity**, **ionisation parameter**, and **environmental classification**.

This is a **catalogue data release** — the underlying MUSE mosaics and emission-line maps were delivered as part of the initial PHANGS–MUSE data release — comprising a **comprehensive source catalogue** of spatially resolved nebular emission regions. These sources span diverse physical environments across the disks of 19 galaxies. Each catalogue entry includes **emission-line fluxes**, **line kinematics**, **extinction estimates**, and **derived quantities** such as gas-phase metallicity and ionisation parameter.

The catalogue enables **systematic studies of individual nebulae** and their role in the interstellar medium (ISM), providing a foundation for investigating **stellar feedback**, **chemical enrichment**, and **environmental trends** both within and across galaxies. It is particularly well-suited to analyses of **spatial variations** in nebular properties across galactic structures (e.g. bars, arms, centres), **metallicity gradients**, and the **influence of galactic dynamics on star formation**.

By combining this detailed nebular catalogue with the broader **PHANGS multi-wavelength framework**—including **ALMA maps of molecular clouds**, **HST imaging of stellar clusters**, and **JWST observations of embedded star formation and dust emission**—this release facilitates a **holistic, multi-scale analysis** of the star formation cycle in the local Universe.

Overview of PHANGS-MUSE Observations

[See inital PHANGS Data Release]

The PHANGS–MUSE survey is a cornerstone of the multi-wavelength PHANGS collaboration, which aims to build a comprehensive view of the star formation process across nearby galaxy (see Emsellem et al. 2022). This data release is based on MUSE integral field spectroscopic observations of 19 nearby star-forming disk galaxies (see **Figure 1**), selected to span a representative range in stellar mass, morphology, inclination, and star formation activity. The majority of the observations were obtained through the PHANGS–MUSE Large Programme (ESO 1100.B-0651; PI Schinnerer), with additional data from pilot programmes 094.C-0623, 095.C-0473 and 098.C-0484, and archival ESO programmes (094.B-0321, 099.B-0242, 0100.B-0116, 098.B-0551, 097.B-0640).

Each galaxy was observed using multiple overlapping pointings with the MUSE integral field spectrograph at the VLT, operated in Wide Field Mode (4750 – 9350 Å) to construct mosaics of the central star-forming disk out to 0.5 – 1.0 $R_{(25)}$. These mosaics typically span 1′ – 3′, corresponding to physical scales of 2 – 10 kpc, and achieve a spatial resolution of ∼100 pc or better under typical seeing conditions of 0.7″ to 1.0″. Adaptive optics (AO) were employed for several more distant galaxies to enhance resolution. All data products were astrometrically aligned and photometrically calibrated using ancillary R-band imaging, with careful PSF homogenization across pointings and wavelengths.

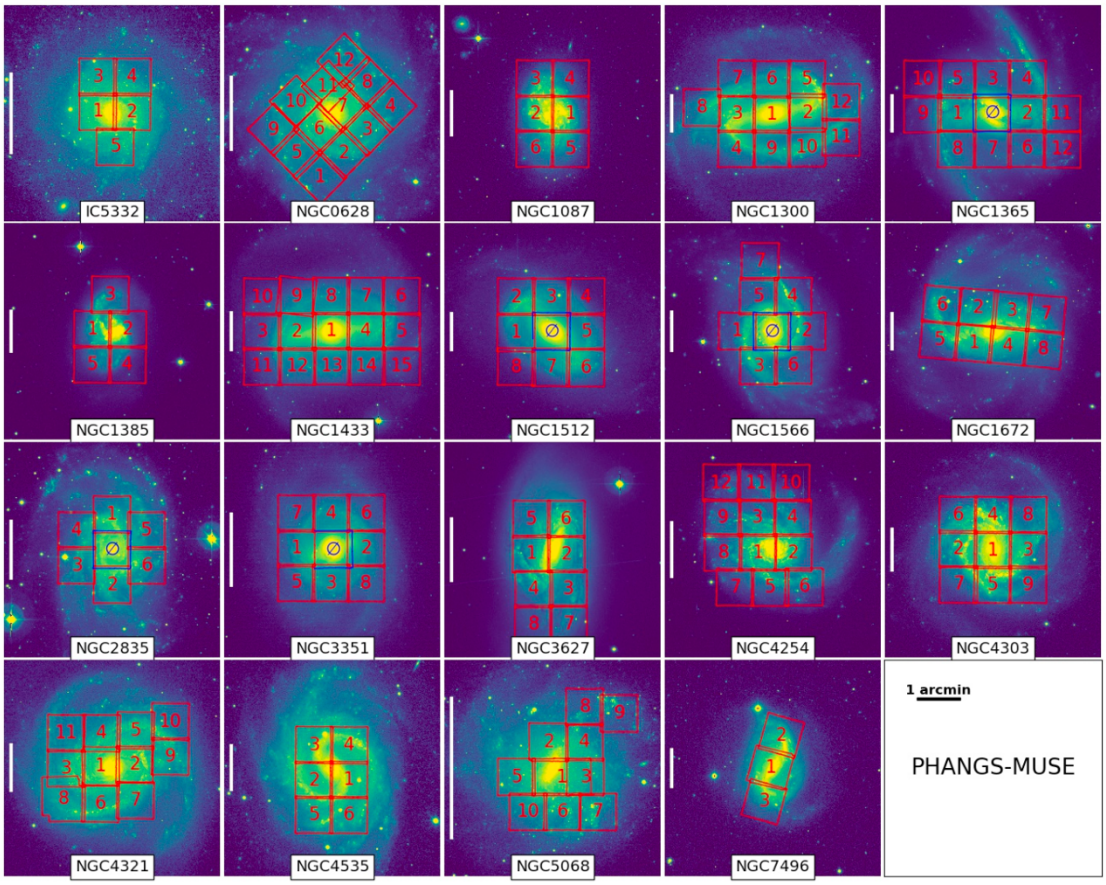


Figure 1: *Footprints for the MUSE observations of PHANGS galaxies. Each panel shows one galaxy from the PHANGS–MUSE sample, displayed over a 5 × 5 arcminute field of view using WFI Rc-band images (or r-band du Pont images for NGC 7496). The footprints of the MUSE exposures are overlaid in red. Pointings marked with the Ø symbol — visible in NGC 1365, NGC 1512, NGC 1566, NGC 2835, and NGC 3351 — and outlined in blue correspond to observations taken outside the main PHANGS campaign. These were reduced using the same data processing pipeline and are included in the PHANGS–MUSE release. A vertical white bar on the left side of each panel indicates a scale of 5 kiloparsecs.*

Table 1: *Overview of the PHANGS galaxies.*

Name	Dist. (Mpc) (a)	v_{sys} (km/s) (b)	PA (deg) (c)	i (deg) (c)	M_* $\log(M_\odot)$ (d)	R_{25} (′) (b)	r_{eff} (′)	$E(B-V)_{MW}$ (mag) (e)	Res. (pc)
IC5332	9.0	699	74.4	26.9	9.67	3.0	1.4	0.014	45
NGC0628	9.8	651	20.7	8.9	10.34	4.9	1.4	0.061	42
NGC1087	15.9	1502	359.1	42.9	9.93	1.5	0.7	0.030	71
NGC1300	19.0	1545	278.0	31.8	10.62	3.0	1.2	0.026	62
NGC1365*	19.6	1613	201.1	55.4	10.99	6.0	3.3	0.018	84
NGC1385	17.2	1477	181.3	44.0	9.98	1.7	0.7	0.017	96
NGC1433*	18.6	1057	199.7	28.6	10.87	3.1	0.8	0.008	83
NGC1512	18.8	871	261.9	42.5	10.71	4.2	0.9	0.009	96
NGC1566*	17.7	1483	214.7	29.5	10.78	3.6	0.6	0.008	76
NGC1672*	19.4	1318	134.3	42.6	10.73	3.1	0.6	0.020	73
NGC2835	12.2	867	1.0	41.3	10.00	3.2	0.9	0.086	33
NGC3351	10.0	775	193.2	45.1	10.36	3.6	1.0	0.024	43
NGC3627*	11.3	715	173.1	57.3	10.83	5.1	1.1	0.029	69
NGC4254	13.1	2388	68.1	34.4	10.42	2.5	0.6	0.033	61
NGC4303*	17.0	1560	312.4	23.5	10.52	3.4	0.7	0.019	96
NGC4321	15.2	1572	156.2	38.5	10.75	3.0	1.2	0.023	59
NGC4535	15.8	1954	179.7	44.7	10.53	4.1	1.4	0.017	80
NGC5068	5.2	667	342.4	35.7	9.40	3.7	1.3	0.090	23
NGC7496*	18.7	1639	193.7	35.9	10.00	1.7	0.7	0.008	104

Notes: Distances are taken from the compilation of Anand et al. (2021) (a). Systemic velocities and optical radii (R_{25}) are from LEDA (Makarov et al. 2014) (b). Position angles and inclinations are based on CO(2–1) kinematics from Lang et al. (2020) (c). Stellar masses were derived by Leroy et al. (2021) using *GALEX* UV and *WISE* IR photometry (d). Foreground extinction values are from Schlafly & Finkbeiner (2011) (e). For NGC 1365, r_{eff} is derived from the stellar scale length (l_*) as $r_{eff} = 1.41 \times l_*$, due to AGN contamination in the photometric fit, following Equation 5 in Leroy et al. (2021) (f). Galaxies marked with an asterisk (*) are classified as AGN by Véron-Cetty & Véron (2010).

Both native-resolution and convolved ("copt") datacubes are provided in the initial data release, the latter having Gaussian PSFs matched across the full field for consistent analysis – and indeed used for this release of the nebulae catalogue.

The PHANGS–MUSE dataset yields spatially resolved emission-line and stellar kinematic maps, calibrated datacubes, and derived physical parameters, forming the basis for high-resolution studies of the interstellar medium, star formation, and feedback processes. This supports both detailed studies within individual galaxies and comparative analyses across the broader PHANGS sample. Key physical properties of the 19 galaxies included in the survey are summarised in **Table 1**.

Overview of PHANGS-MUSE Nebula Catalog

This data release includes a catalogue of 31,399 sources (30,790 of which are ionized nebulae) identified across 19 nearby star-forming galaxies observed with MUSE as part of the PHANGS–MUSE survey. Nebulae were detected from Hα surface brightness maps using a modified version of the HIIphot algorithm, which was adapted for integral field spectroscopic data by incorporating associated error maps and removing the need for continuum subtraction from broad-band imaging. The detection threshold was set to 3σ above a locally estimated background, with a terminal gradient of 5.0 EM pc^{-1} (where the emission measure, EM, is in cm^{-6} pc) used to define nebular boundaries, corresponding to 2.43×10^{-16} erg s^{-1} $arcsec^{-2}$ pc^{-1} for all galaxies. This threshold ensures consistent detection sensitivity across systems with varying resolution. To avoid spurious detections, the algorithm applied spatial smoothing over three iterations, limited the minimum S/N for flux integration, and trimmed initial detections using

an isophotal boundary at 50% of the internal median Hα surface brightness. For full information see Santoro et al. (2022) and Groves et al. (2023).

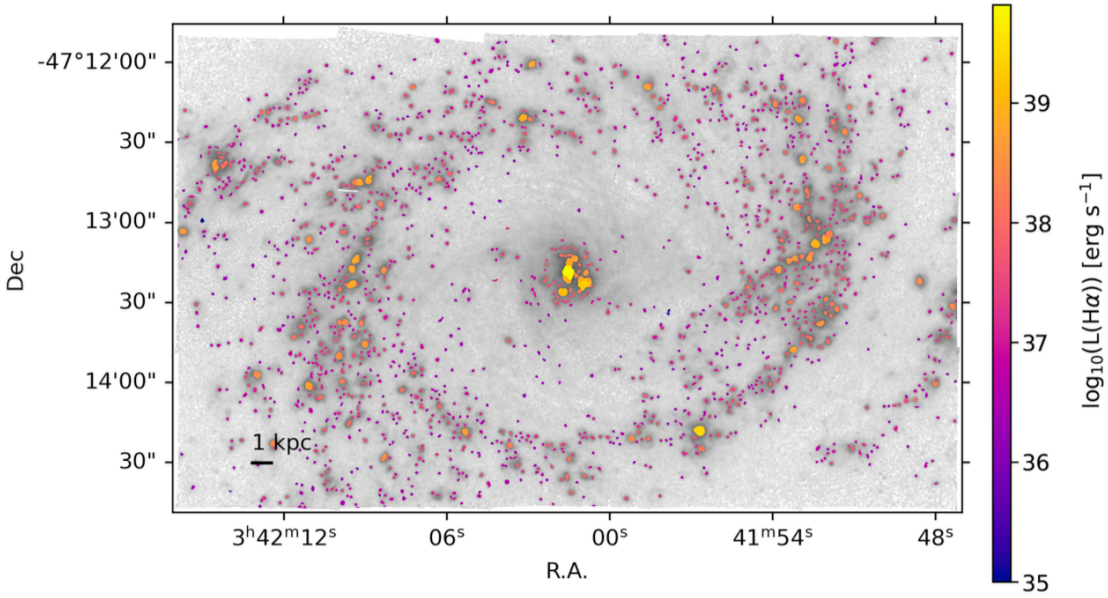


Figure 2: *A visualisation of the two-dimensional spatial extent and distribution of all nebulae in the galaxy NGC 1433. The background greyscale image shows the Hα emission in logarithmic scale, while the colour of each nebula indicates its intrinsic (dust-corrected) Hα luminosity*

Once nebulae were segmented, integrated spectra were extracted from the native-resolution, unconvolved mosaicked datacubes, avoiding artificial smearing from PSF homogenization. Emission lines were then re-fit using the PHANGS-MUSE Data Analysis Pipeline (DAP), extending the standard fitting range to include the [S III] λ9068 line. Spectral fitting employed single Gaussian profiles for all lines, grouping them into hydrogen, low-ionization, and high-ionization species. Line velocities are reported relative to each galaxy's systemic velocity, and the Milky Way foreground extinction was corrected using Schlafly & Finkbeiner (2011) maps with the O'Donnell (1994) extinction law (R_V = 3.1). Measured emission-line fluxes were corrected for extinction via the Balmer decrement, assuming an intrinsic Hα/Hβ ratio of 2.86. This methodology allows for robust, aperture-independent measurements of key lines including Hα, Hβ, [O III], [N II], and [S II]. The catalogue also includes derived properties such as V-band attenuation (A_V), equivalent widths (both raw and continuum-subtracted), gas-phase metallicities using strong-line calibrators (e.g. Scal-PG16), and ionization parameters based on [S III]/[S II] ratios (see also Groves et al. 2025).

These procedures initially identified 31,497 nebulae with well-defined spatial boundaries. During catalogue cleaning, 98 sources overlapping with Gaia DR2 foreground star masks were removed entirely due to likely contamination from stellar continuum (Emsellem et al. 2022, §5.3). An additional 609 nebulae with centroids located within one PSF FWHM of the mosaic edges are retained in the catalogue, but flagged due to potential truncation of their boundaries and underestimation of their total fluxes. These flagged edge sources remain useful for many applications, but should be treated with caution in analyses sensitive to morphology or integrated luminosity. The resulting catalogue contains 31,399 sources, of which 30,790 are unflagged (FLAG_EDGE=0) and represent the core science-quality sample of ionized nebulae.

A visualization of the nebular catalogue in one of the galaxies, NGC 1433, is shown in **Figure 2**, where the distribution and extent of H II regions are overlaid on the Hα emission map. The color of each nebula encodes its dust-corrected Hα luminosity, illustrating the power of the catalogue to trace the intensity and spatial structure of star formation across galactic environments.

The underlying astrometric calibration is based on alignment to Gaia DR2 using R-band reference images (Razza et al., in prep.), and is accurate to <0.05 arcsec across the mosaics. Photometric calibration was performed using matched R-band imaging and zero-points derived from Gaia-based reference photometry, following procedures described in Emsellem et al. (2022). MUSE data were reduced with the official pipeline (Weilbacher et al. 2020), and sky subtraction and flux normalization were refined using broad-band image comparison and regression-based corrections. No illumination correction was necessary due to the use of integral field data.

The sky coverage consists of MUSE mosaics covering the central star-forming disks of 19 galaxies, with no internal gaps due to overlapping exposures. Each mosaic typically spans 1 to 3 arcmin, corresponding to a total mapped area of approximately 0.15 square degrees. Detection was performed in the Hα band, extracted from the MUSE datacubes; no multi-band detection image was used.

The limiting sensitivity of the catalogue corresponds to Hα luminosities of approximately 10^{36} erg s^{-1}, equivalent to the ionizing output of a single O7V star (see Santoro et al. 2022), and extends up to a maximum luminosity of $\sim 10^{40}$ erg s^{-1}. Catalogue completeness exceeds 95% for Hα-emitting spaxels within 0.5 $R_{(25)}$ above the 3σ detection threshold. The limiting depth is broadly uniform across the mosaics, with only minor variations introduced by differences in exposure time and seeing conditions.

The total number of sources is 30,790, distributed across 19 galaxies, with per-galaxy counts ranging from a few hundred to over 3,000. The catalogue and nebular mask files total 39 FITS files (catalog and masks – see below), with a combined volume of around 185 MB.

File Types

This data release includes two types of FITS files per galaxy, each following a standardized naming convention. **Functionally, the catalogue is designed to be queried as a single, unified dataset**—with all nebulae across the 19 galaxies presented in a common format within a logically continuous table. **Practically, however, the catalogue is organized as a set of per-galaxy "tiles"**, with one source catalogue and **one corresponding nebular mask per galaxy**.

Source Catalogue Files

- **Filename:** {galaxy_name}_catalog.fits
- **Description:** FITS binary tables containing the list of nebulae detected in the galaxy, along with their derived physical properties (e.g., emission-line fluxes, velocities, metallicities, attenuation, environment classification).
- **Example:** NGC1365_catalog.fits

Nebular Mask Files

- **Filename:** {galaxy_name}_nebulae_mask.fits
- **Description:** FITS images where each pixel value corresponds to the ID of the nebula it belongs to, enabling mapping and visualization of nebular regions across the galaxy. Pixels not associated with any nebula have a value of -1.
- **Example:** NGC1365_nebulae_mask.fits

Naming Convention

- {galaxy_name} refers to the uppercase galaxy name with no spaces (e.g. NGC4321, IC5332).
- All filenames are lowercase with underscores separating components.
- All files use the **FITS format** and comply with ESO Phase 3 data standards.

This naming scheme is designed to facilitate automated parsing and matching of catalogue and mask files on a per-galaxy basis.

Catalogue Columns

Table 2: *Columns in the catalogue.*

Column	Unit	Description
SOURCE_ID	—	Unique source identifier (gal_name+region_ID)
GAL_NAME	—	Galaxy name
REGION_ID	—	Region ID
CEN_RA	deg	RA (J2000), center weighted by Hα intensity
CEN_DEC	deg	Dec (J2000), center weighted by Hα intensity
FLAG_EDGE	—	Flag set to 1 if region is within one PSF of field edge
FLAG_STAR	—	Flag set to 1 if overlapping with a foreground star
DEPROJ_R_R25	R25	Deprojected galactocentric distance in units of R25
DEPROJ_R_REFF	r_eff	Deprojected galactocentric distance in units of effective radius
DEPROJ_PHI	deg	Deprojected azimuthal angle in galaxy plane
REGION_AREA	pixels	Area of the nebular region in pixels
EMLINE*_FLUX	1e-20 erg/s/cm²	Emission line fluxes (see emission line table)
EMLINE*_FLUX_CORR	1e-20 erg/s/cm²	Attenuation-corrected emission line fluxes using O'Donnell (1994), RV = 3.1
EMLINE*_VEL	km/s	Line velocity relative to systemic velocity
EMLINE*_SIGMA	km/s	Velocity dispersion, corrected for instrumental broadening
AV	mag	V-band attenuation from Balmer decrement, assuming O'Donnell (1994), RV = 3.1
EW_HA6562_RAW	Å	Hα equivalent width, direct measurement
EW_HB4861_RAW	Å	Hβ equivalent width, direct measurement
EW_HA6562_FIT	Å	Hα equivalent width, after stellar continuum subtraction
EW_HB4861_FIT	Å	Hβ equivalent width, after stellar continuum subtraction
HA6562_LUM_CORR	erg/s	Attenuation-corrected Hα luminosity
BPT_NII	—	BPT classification (based on [N II])
BPT_SII	—	BPT classification (based on [S II])
BPT_OI	—	BPT classification (based on [O I])
MET_SCAL	—	Metallicity using the Pilyugin & Grebel (2016) Scal calibration
DELTA_MET_SCAL	—	Offset from radial metallicity gradient
LOGU	—	Ionization parameter from [S III]/[S II], following Díaz et al. (1991)
ENVIRONMENT	—	Environment flag (e.g., arm, interarm, bar; see environment table)

Table 3: *Emission line table. Wavelengths and ionisation potential of the relevant ion for each emission line included in the public catalog. All lines are corrected for the Milky Way foreground dust extinction. Wavelengths are taken from the National Institute of Standards and Technology (NIST) and are Ritz wavelengths in air (consist with wavelengths in the public data release) except for the H Balmer lines, in which case we use the 'observed ' wavelength in air as reported in NIST. The DAP string name is used to identify the correct extension in the PHANGS-MUSE MAPS files. Ionisation potentials are taken from Draine (2011).*

Line Name	Wavelength (air) [Å]	String ID	Ionization Potential [eV]	Fixed Ratio
Hydrogen Balmer lines				
Hβ	4861.35	HB4861	13.60	no
Hα	6562.79	HA6562	13.60	no
Low ionisation lines				
[O I] λ6300	6300.30	OI6300	—	no

[N II] λ6548	6548.05	NII6548	14.53	0.34 × [N II] λ6584
[N II] λ6584	6583.45	NII6583	14.53	no
[S II] λ6717	6716.44	SII6716	10.36	no
[S II] λ6731	6730.82	SII6730	10.36	no
High ionisation lines				
[O III] λ4959	4958.91	OIII4958	35.12	0.35 × [O III] λ5007
[O III] λ5007	5006.84	OIII5006	35.12	no
[S III] λ9068	9068.6	SIII9068	23.34	no

***Table 4**: BPT flags included in the catalog.*

Column Name	Value	Meaning
BPT_NII	0	Star formation
	–1	Low S/N < 5
	1	Composite
	3	AGN
BPT_SII	0	Star formation
	–1	Low S/N < 5
	2	LI(N)ER
	3	AGN
BPT_OI	0	Star formation
	–1	Low S/N < 5
	3	AGN

***Table 5:** Our Environmental flags, based on simplified assignments from Querejeta et al. (2021).*

Label	Original Environment (Querejeta2021)	Mapped Environment
1	Centre	Centre
2	Bar (excluding bar ends)	Bar
3	Bar ends	Bar
5	Spiral arms inside interbar region (R_gal < R_bar)	Arm
6	Spiral arms (R_gal > R_bar)	Arm
4	Interbar region (R_gal < R_bar)	Interarm
7	Interarm (R_gal > R_bar)	Interarm
8	Outer disc (R_gal > end of spiral arms)	Interarm
9	Disc (R_gal > R_bar) in galaxies without spiral masks	Disc

Programmatic Access

The PHANGS–MUSE Nebular Catalogue is available through the **ESO Science Archive** and can be queried using the **Table Access Protocol (TAP)** service at:

https://archive.eso.org/tap

The catalogue can be accessed programmatically using tools like **TOPCAT**, **ADQL**, **pyvo**, or **astroquery**. Below are a couple examples.

Query available columns in the catalogue (see here):

```
SELECT column_name, datatype, unit, ucd
from TAP_SCHEMA.columns
where table_name='PHANGS_DR1_NebCat'
```

Select regions in NGC 1433 not flagged as near the edge (see here):

```
SELECT REGION_ID, RAJ2000, DECJ2000
FROM PHANGS_DR1_NebCat
WHERE GAL_NAME = 'NGC1433'
AND FLAG_EDGE = 0
```

Query for the most Halpha luminous regions across all galaxies (see here):

```
SELECT GAL_NAME, REGION_ID, HA6562_LUM_CORR
FROM PHANGS_DR1_NebCat
WHERE FLAG_EDGE = 0
AND HA6562_LUM_CORR > 1e40
```

For a full description of the catalogue columns, units, and UCDs, see the accompanying documentation or explore the metadata through the TAP service.

Acknowledgements

PHANGS-MUSE was only possible through the dedicated effort of several people close to a decade. Users of this dataset are requested to cite the following scientific publications associated with the data:

- **Santoro et al. (2022), Groves et al. (2023, 2025)** – for the PHANGS–MUSE Nebular Catalogue and the methodology used to generate and analyze the catalogue.
- **Emsellem et al. (2022)** – for the PHANGS–MUSE survey design, observations, and data reduction pipeline.

The PHANGS–MUSE observations were conducted under ESO programmes 1100.B-0651, 095.C-0473, 094.C-0623, and 098.C-0484, and include archival data from 094.B-0321 (MAGNUM), 099.B-0242, 0100.B-0116, 098.B-0551 (MAD), and 097.B-0640 (TIMER).

According to the Data Access Policy for ESO data held in the ESO Science Archive Facility, all users are required to acknowledge the source of the data with appropriate citation in their publications. Since processed data downloaded from the ESO Archive are assigned Digital Object Identifiers (DOIs), the following statement must be included in all publications making use of them:

- Based on data obtained from the ESO Science Archive Facility with DOI: https://doi.org/10.18727/archive/47, and on data products produced by the PHANGS consortium.

Publications making use of data which have been assigned an archive request number (of the form XXXXXX) must also include the following statement in a footnote or in the acknowledgement:

- Based on data obtained from the ESO Science Archive Facility under request number <request_number>.

Science data products from the ESO archive may be distributed by third parties, and disseminated via other services, according to the terms of the Creative Commons Attribution 4.0 International license. Credit to the ESO provenance of the data must be acknowledged, and the file headers preserved.

References

Anand, G. S., Lee, J. C., Van Dyk, S. D., et al. 2021, MNRAS, 501, 3621
Draine B. T., 2011, Physics of the Interstellar and Intergalactic Medium. Princeton University Press
Emsellem E., et al., 2022, A&A, 659, A191
Groves, B., Kreckel, K., Santoro, F., et al. 2023, MNRAS, 520, 4902
Groves, B., Kreckel, K., Santoro, F., et al. 2025, MNRAS, 539, 1850
Lang, P., Meidt, S. E., Rosolowsky, E., et al. 2020, ApJ, 897, 122

Leroy, A. K., Schinnerer, E., Hughes, A., et al. 2021, ApJS, 257, 43
O'Donnell J. E., 1994, ApJ, 422, 158
Makarov, D., Prugniel, P., Terekhova, N., Courtois, H., & Vauglin, I. 2014, A&A, 570, A13
Santoro F., et al., 2022, A&A, 658, A188
Schlafly, E. F. & Finkbeiner, D. P. 2011, ApJ, 737, 103
Querejeta M., et al., 2021, A&A, 656, A133
Véron-Cetty M. P., Véron P., 2010, A&A, 518, A10